NANO LETTERS

Letter

pubs.acs.org/NanoLett

Dynamic and Electronic Transport Properties of DNA Translocation through Graphene Nanopores

Stanislav M. Avdoshenko,[†] Daijiro Nozaki,[‡] Claudia Gomes da Rocha,*[,¶] Jhon W. González,[§] Myeong H. Lee,[∥] Rafael Gutierrez,[‡] and Gianaurelio Cuniberti[‡]

[†]School of Materials Engineering, Purdue University, West Lafayette, Indiana, United States

[‡]Institute for Materials Science and Max Bergmann Center of Biomaterials, TU Dresden, 01062 Dresden, Germany

[¶]Nanoscience Center, Department of Physics, University of Jyväskylä, 40014 Jyväskylä, Finland

[§]International Iberian Nanotechnology Laboratory, Avenido Mestre José Veiga, 4715-330, Braga, Portugal

[∥]Department of Chemistry, University of Michigan, Ann Arbor, Michigan 48109, United States

ABSTRACT: Graphene layers have been targeted in the last years as excellent host materials for sensing a remarkable variety of gases and molecules. Such sensing abilities can also benefit other important scientific fields such as medicine and biology. This has automatically led scientists to probe graphene as a potential platform for sequencing DNA strands. In this work, we use robust numerical tools to model the dynamic and electronic properties of molecular sensor devices composed of a graphene nanopore through which DNA molecules are driven by external electric fields. We performed molecular dynamic simulations to determine the relation between the intensity of the electric field and the translocation time spent by the DNA to pass through the pore. Our results reveal that one can have extra control on the DNA passage when four additional graphene layers are deposited on the top of the main graphene platform containing the pore in a 2 × 2 grid arrangement. In addition to the dynamic analysis, we carried electronic transport calculations on realistic pore structures with diameters reaching nanometer scales. The transmission obtained along the graphene sensor at the Fermi level is affected by the presence of the DNA. However, it is rather hard to distinguish the respective nucleobases. This scenario can be significantly altered when the transport is conducted away from the Fermi level of the graphene platform. Under an energy shift, we observed that the graphene pore manifests selectiveness toward DNA nucleobases.

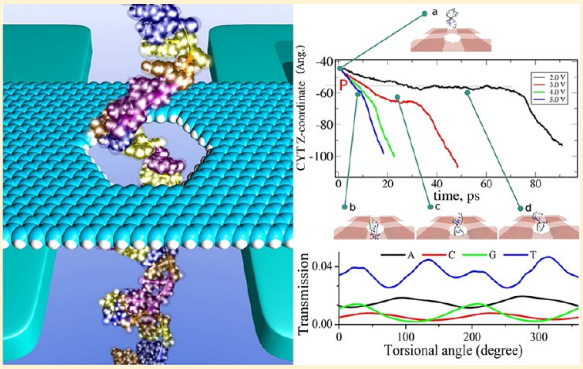

KEYWORDS: *Graphene, DNA sequencing, nanopores, biosensors*

The search for effective techniques for precisely tracking DNA sequences has become an active research field that can promote important technological innovations in diagnostics, forensic biology, and biotechnology branches. DNA, the biopolymer composed of four nucleotide units [adenine (A), cytosine (C), guanine (G), and thymine (T)], carries the genetic information of all living beings and deciphering its sequence became one of the biggest challenges in modern science.[1] Only the human genome, for example, is composed of over 3 billion base pairs and its complete identification demands the manipulation of reliable and rapid large-scale sequencing methods.[2,3] Several techniques for DNA sequencing have been proposed since the first attempts developed by Maxam et al.[4] and Sanger et al.[5] in the 1970s. In particular, Sanger method uses modified nucleotide bases, named dideoxynucleotides triphosphates, as DNA chain terminators that can be subsequently distinguished via gel electrophoresis technique. Nevertheless, less invasive methods that do not involve the manipulation of complex chemical reactions are in high demand. In addition, Sanger method might not be a reliable tool for encoding repetitive DNA units that are larger than the typical Sanger read length (~700 bp fragments).

A promising alternative for accurate and low-cost DNA readouts has been explored by means of single-molecule sequencing techniques using artificial nanopore membranes mostly fabricated via ion/electron beam techniques. Biological nanopores generated with α-hemolysin protein were used to map the DNA sequence as the molecule translocates through it.[6,7] New venues are being opened with recent implementations of solid-state nanopores[8,9] made of synthetic materials such as SiNx,[10,11] SiO_2[12−14] and Al_2O_3[15] membranes. Regardless of the main chemical/physical features of the detecting pore, its basic sequencing procedure consists of driving the molecule along its open area by means of an applied electric field. The membrane separates two reservoirs containing electrolytic solution in which the electric field is applied forcing the DNA to move

Received: December 22, 2012
Revised: April 15, 2013
Published: April 15, 2013

through the pore. The ionic current is hence measured in real time as the molecule flows through the vacancy of the pore. Eventually one can observe abrupt drops in the ionic current associated with a partial obstruction in the flow of ions in response to the DNA translocation. In principle, each nucleotide can disrupt the ionic current in a distinguishable way and, as a result, the sequencing can be disclosed. Other prominent attempts for DNA sequencing technology were realized adopting electron tunneling as readout mechanism. Nanogap architectures[16,17] synthesized via functionalized or configurable electrodes[18] were implemented for sequencing single nucleotides by direct measurements of tunneling currents. Anyhow, nanopore methods rely on the principle that each nucleotide has a particular size and shape, producing then different readings on the nanocircuits. Each nucleotide unit can generate a certain electrical signal that can be detected in real-time experiments. Nevertheless, the success of such measurements depends extremely on attaining single-base resolution and this is not easy to achieve. The shape of the nanopore/nanogap itself is one of the first concerns that must be taken into account since it can heavily affect the performance of the device.[19,20] In particular, the thickness of the detecting platform can play a major role in recognizing the individual DNA bases. The deeper the thickness of the pore is, the more difficult it is to probe the local structure of the molecule as it travels through the channel. At this point, it seems straightforward to speculate that perhaps graphene,[21] the one-atom-thick carbon layer packed onto a honeycomb lattice, might be a good platform for DNA sensing since they are known to be the thinnest material ever measured. Besides, graphene exhibits remarkable conducting and mechanical properties[22] that already guided many scientific groups to demonstrate their use as nanopore sensors.

The pioneer experimental realizations in this field were conducted independently in the groups led by Golovchenko,[23] Dekker,[24] and Drndić[25] where one could measure variations in the ionic current as the DNA is driven through the graphene pore. Nonetheless, before assuring that graphene nanopores are indeed a suitable material for reading DNA molecules, several physical aspects must be carefully checked. For instance, one must evaluate the optimal speed, frequency, and the orientation of the DNA strand as it threads the pore, the geometry of the pore, the DNA−pore interaction, and even how the potential of the membrane influences the DNA translocation. Such multitude of effects can induce ambiguous interpretations of how efficient this sequencing technique can actually be. Further issues such as the suppression of spurious signals originated from stochastic motions of the DNA embedded in the fluid or occasional overlaps of the response associated with different nucleobases must be resolved for turning this sequencing approach more practical.[26] In order to assist experimentalists in overcoming these obstacles, a more complete theoretical understanding is highly demanding.

Many theoretical works have already addressed such intriguing phenomenon and they show that graphene nanopores are suitable platforms for scanning DNA information with molecular resolution. Semiclassical approaches,[17] or first principle transport calculations[27] were employed to verify the feasibility of graphene nanopores in sequencing DNA strands. One reported that the presence of a nucleobase in the graphene nanopore strongly affects the charge density in the vicinity of the opened area, inducing thereby current variations of the order of microamperes at bias voltages of 0.1 V.[28] Although the calculations conducted in the referred work were carefully performed via nonequilibrium Green functions method combined with density functional theory (DFT), the graphene nanopores considered as target systems have extremely small radius (~0.6 nm), a factor that certainly plays an important role in the amplification of the graphene sensitivity to DNA. In another kind of framework, one assumed a simplified picture for computing the electronic current along the nanopores by integrating directly the density of states.[29] Still, a full ab initio description employed to derive the electronic transport properties of more realistic graphene nanopores is missing and our goal is exactly to bridge this gap in the field. We performed a robust theoretical analysis about the transport response of graphene nanopores when DNA strands translocate through it. Our results reveal that the conductance of the graphene pore does not experience pronounced changes in response to the presence of the target molecule because its saturated edges can screen the influence of the DNA. This picture can be modified when the electronic transport is conducted at energies shifted from the Fermi level of the graphene sensor. In this regime, the sensor acquires selectiveness with respect to which nucleobase is coplanar to the graphene plane. Additional information was also extracted by carrying out classical nonequilibrium molecular dynamics simulations to investigate the dynamical trajectory developed by the DNA as it translocates through the pore with the aid of a driven electric field. We designed a different detection setup in which four additional graphene plates are deposited on top of the main graphene platform containing the pore (see Figure 1). This new arrangement provides extra control on the DNA passage and reduces the kinetic motion of the carbon atoms located on the edges of the pore.

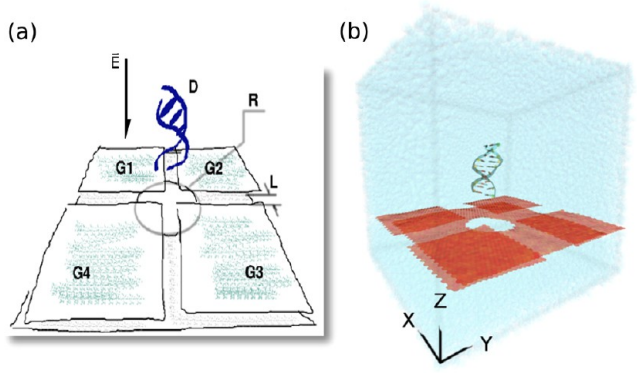

Figure 1. (a) Schematic representation of a graphene nanopore of radius R with four extra graphene sheets labeled as G1, G2, G3, and G4 used to retard the translocation fly of the DNA molecule (D). $\vec{E}$ is the driven electric field applied to force the DNA passage. (b) Original atomic structure of our model system inserted in water solution.

Dynamical Aspects. We performed a detailed theoretical analysis including transport and dynamical aspects of the translocation of DNA molecules through an artificial graphene nanopore. We begin by presenting the studies carried on via classical molecular dynamic (MD) simulations that provide crucial information about the permeation of double-stranded DNA (ds-DNA), 5′-CCAAGCTTGG-3′, molecules through the pore. One can also infer how geometrical aspects of the atomic structures influence the translocation processes. A schematic representation of the system can be seen on Figure 1

that consists of a graphene surface with a pore of radius $R \sim 6$ nm on its center. The dimensions of our "model pore" is in accordance with experimental realizations which are capable of sculpturing holes ranging 5−10 nm in diameter.[30] Furthermore, four smaller sheets, referred here as gates G1, G2, G3, and G4, are arranged over the main platform containing the pore. The plates form a cross-shaped gap in which its center is aligned with the pore. This particular setup aids in the reduction of the DNA translocation velocity since they can exert extra friction forces capable of retarding the process. As suggested by Wells et al.,[31] it is possible to achieve a certain degree of control on the DNA conformation by engineering the nanopore surface. It is also feasible to diminish the permeation velocity by increasing the viscosity of the fluid that drags the DNA through the pore.[32] However such reduction is sometimes not sufficient. The gates also suppress considerably the kinetic motion of the atoms disposed along the pore-edge that might benefit the transport measurements due to noise reduction. Such bilayer-pore configuration could be fabricated by means of sophisticated etching techniques as the one carried by Shi et al.[33] from which two distinct patterned graphene layers could be synthesized and placed together. The graphene membranes are placed in a box of volume 10^3 nm^3 filled with water molecules. On the limits of the box, the whole graphene platform and the four extra membranes are treated under zero force regime; as for the aqueous environment, we apply periodic boundary conditions. The gate grids were arranged in the following two different manners: (i) with a wider opening where the smallest distance between the gates is $L \sim 3$ nm and (ii) with a narrower constriction where $L \sim 2$ nm.

A ds-DNA containing 10 bp is initially situated right on top of the pore. In particular for the ds-DNA, most of its mechanical and electrical properties come from its characteristic double-helical shape and from its charged phosphate backbone. Under the presence of an external electric field acting on its negatively charged segments, the molecule is drifted through the hole together with water molecules and ions. The whole system (graphene membranes plus DNA) contains approximately 200K atoms and was treated within molecular dynamics framework using NAMD2 code.[34,35] The parametrization scheme was written in CHARMM format[36] based on AMBER99[37] and TIP3P[38] force field approximations using VEGAZZ.[39] The system was equilibrated from 0 K to room temperature using NVT canonical ensemble with isothermal constraint condition given by Langevin thermostat.[40] The dynamical trajectories are obtained by solving Newton's equation of motion from which dynamical average observables can be extracted. The adopted integration step of the Verlet algorithm was 2 fs for a total time range of 90 ps. After equilibration, the influence of the thermostat can be switched off and the system is kept at room temperature in which an external electric field is applied.

In Figure 2, we tracked the z-coordinate component of a ds-DNA (being the graphene sensor located on xy plane) in time taking as reference point a cytosine unit. A perpendicular electric field providing potential differences from 2 to 5 V drives the molecule through the graphene pore setup. The insets depict four different snapshots of the system while the molecule passes through the graphene hole. It is straightforward to notice through the insets the remarkable elastic properties of the whole graphene support that pronouncedly bends along the translocation direction of the DNA. The gray horizontal line (P) on the mainframe marks the position of the pore. One can

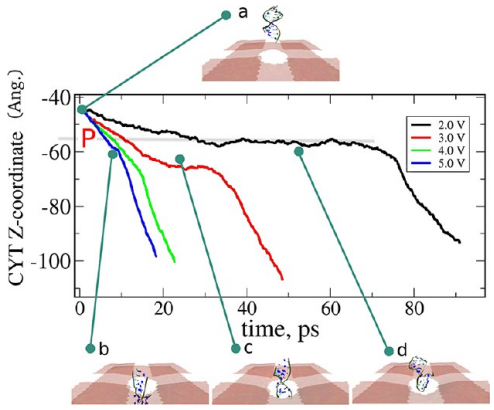

Figure 2. Time evolution of the position along z-component (in angstroms) of a double strand DNA molecule containing 10 bp in total and taking as reference a cytosine base. Different electric potential intensities are established to force the translocation of the DNA through the graphene nanopore. Insets show snapshots taken from the dynamic fly. The gray horizontal line (P) represents the location of the pore.

see that at high electric potential intensities (4 and 5 V), the DNA strand flows at high speed requiring approximately ∼12 ps to complete the whole translocation. As the electric potential is diminished to 3 V, a short delay in the translocation time can be observed. A small plateau on the curve reveals that the molecule gets "trapped" for a while in the vicinity of the pore. This transient state can be highly increased by setting the electric potential at 2 V where the DNA does not have enough propulsion to pass through the pore. The molecule bounces and even folds in the surroundings of the vacancy for approximately ∼60 ps until it finally accomplishes the translocation with velocity of 1 bp/60 ps (≈ 17 bp/ns). This partial impediment of the molecule in overcoming the pore is an important factor which must be considered for achieving optimum DNA sequencing in real-time. This delay must be high enough for the equipment to capture any relevant signal from that particular nucleotide trapped on the pore. The precision in some nanopore measurements can be conducted at minimum pulse durations of the order of 100 μm[25] depending on the type of filter circuit used. Measurements realized in other types of nanopore materials at potential intensities of hundreds of millivolts show speeds of approximately 33 bp/ns[9] that are in rather good agreement with our theoretical prediction.

Delaying the DNA translocation for a certain time has important implications for achieving optimum real-time detection at molecular scale. Now we illustrate its significance by presenting a counter example. At a first glance, one expects that the DNA is a highly ordered spiral molecule that can develop a regular vertical trajectory through the pore. In the experiments designed to sense the DNA via tunneling currents, the profile of the electrostatic potential associated with the molecular structure during its propagation can affect the readings. In this sense, any distinguishable variation in the tunneling currents is simply a result of the (almost) perfect alignment of each individual nucleotide with the carbon atoms of the sensor. The real challenge for the experimentalists is to exactly set proper experimental conditions that will yield a precise single-base reading. Under real experimental conditions, DNA is not a completely perfect helical molecule that will pass vertically undamaged through the pore. It can bend or even fold

dx.doi.org/10.1021/nl304735k | Nano Lett. 2013, 13, 1969−1976

in the pore before completing its path. We repeated the same dynamical simulations conducted previously imposing three disordered initial configurations for the DNA strand that we named as (i) weakly ordered (WO), (ii) disordered (D), and (iii) highly disordered (HD). The level of disorder is dictated by how much the DNA atomic structures deviate from its canonical helical shape such as shown on the insets of Figure 3.

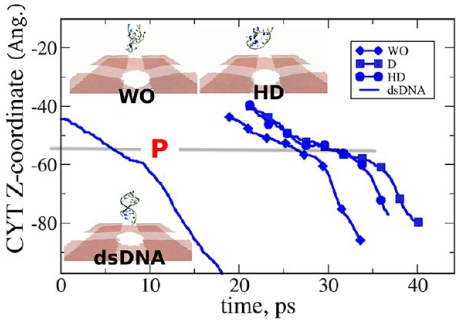

Figure 3. Time evolution of the position along *z*-component (in angstroms) of a double strand DNA molecule containing 10 bp in total and taking as reference cytosine base. Different initial conditions for the DNA are imposed: (ds-DNA) double strand DNA on its canonical helical shape, (WO) weakly disordered, (D) disordered, and (HD) highly disordered. The electric potential is fixed at 5.0 V to force the translocation of the DNA through the graphene nanopore. Insets show some snapshots taken from the dynamic fly. The gray horizontal line (*P*) represents the location of the pore.

The latter also shows the evolution in time of the *z*-coordinate component of the cytosine reference base for the standard ds-DNA spiral and the three other disordered configurations with a fixed driving potential of 5.0 V. As one can see, the dynamical trajectories for the ordered and disordered cases do not differ, revealing that the nucleobases cannot be distinguished by monitoring in real time their translocation (although their molecular structures are considerably different). The electric field intensity is high enough to speed up the molecule translocation without delays. The DNA dynamics along *z*-axis is independent of its atomic arrangement. This is a situation in which there is no certainty that a continuous single-base detection can be conducted by the graphene sensor. In other words, if DNA translocates directly through the pore without any delays, it is highly probable that the sensor will misread its structure since its kinetic trajectory is not related to its molecular details.

Electronic Results. Certainly all the dynamical aspects discussed up to now are relevant to shed light on the enigma surrounding DNA sequencing through graphene nanopores. Nevertheless, it is also essential to present reliable theoretical results about their electronic response which is the main readout scheme we consider for our sensor devices. For such analysis, the four extra graphene gates used to retard the translocation of the DNA and suppress the kinetic noise are removed since the transmission will be computed solely along the main platform containing the pore. These four extra graphene sheets are part of the electrodes that are embedded in our description throughout self-energy terms. Under static conditions, the overall transport profile of the systems will not be heavily affected upon atomistic discrepancies originated from the electrode elements. Besides the removal of the extra graphene sheets, we also eliminate spurious signals originated from edge-disorder along the pore. In this sense, the schematic of the pore was considerably simplified. The model pore has a hexagonal shape and is sculptured on a graphene zigzag-edge nanoribbon (zGNR) of ∼4.5 nm in width and all its dangling bonds were passivated with hydrogen atoms as depicted in Figure 4. Since zigzag-edge structures are known for their

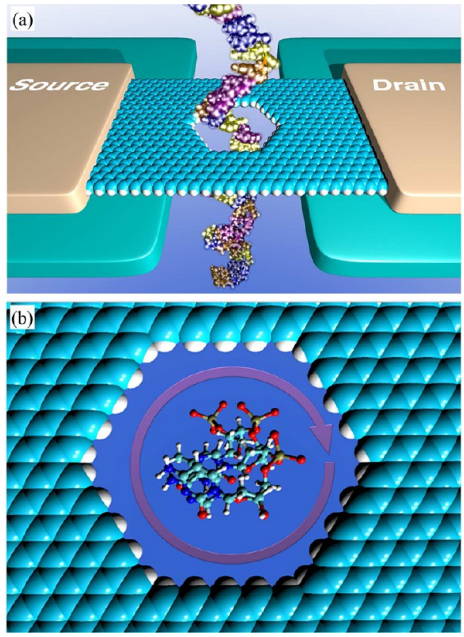

Figure 4. (a) Representation of a graphene nanopore device with dangling bonds saturated with hydrogen atoms through which a DNA molecule moves vertically. (b) The top view of the relaxed nanopore structure containing a DNA segment in which adenine base is aligned with the graphene plane. The transparent arrow indicates how the molecule is rotated on the center of the sensor.

characteristic flat edge-state at the Fermi level, all the atoms along the edge of the pore follow zigzag arrangement. This offers a more promising environment to perceive the DNA molecule located on the vicinity of the pore. The pore is constructed at the center of the ribbon and our calculations were realized in two different platforms: (i) a narrower pore with radius of R_1 = 1.6 nm and (ii) a wider one with R_2 = 2.0 nm. Although the pore sensor was highly simplified for this electronic analysis, their sizes range realistic orders of magnitude. The radius of a DNA helix is ∼1.2 nm and the van der Waals radius of ∼0.2 nm, a minimum size for the nanopore radius would be approximately of 1.2 + 4 × 0.2−1.6 nm. Therefore, here we will deal with graphene nanopore structures of more attainable radius sizes, that is, ≥1.6 nm. Such pore geometry can be designed within the same tailoring techniques mentioned above conducted by Shi and coauthors[33] in which a remarkable control over the edge-formation of the graphene samples was achieved. Their top-down fabrication approach produced several types of graphene nanostructures shaped simply with zigzag terminations.

The electronic transport calculations were done considering a conducting channel composed of a central scattering region (M) connected to left (L) and right (R) electrodes. In the case of nanopore systems, the scattering region comprises the whole defective area of the ribbon and this central section is transparently attached to semi-infinite extensions of the same pristine zigzag ribbon mimicking the electrodes. Its full Hamiltonian is then given by $H = H_M + H_L + H_R + V_L + V_R$

dx.doi.org/10.1021/nl304735k | *Nano Lett.* 2013, 13, 1969−1976

with $V_{L/R}$ being the coupling term between left/right lead and the scattering region. Its electronic structure is obtained through self-consistent density functional-based tight binding (SCC-DFTB) approach,[41,42] which consists of a second-order expansion of the Khon-Sham total energy, treated within DFT, with respect to charge density fluctuations. Prior to the realization of any electronic calculations, all atomic structures were fully optimized using conjugated gradient method.[41] Standard Green function formalism[43] was employed to compute density of states (DOS) and transmission for the isolated pristine and pore-shaped graphene nanoribbons and for the nanopore in the presence of DNA nucleotides. In particular, the conductance along the channel is obtained within coherent regime via Landauer formula[43] where its transmission is expressed in terms of Green functions. The transport response of the systems is hence monitored as a function of energy and other geometrical parameters such as the diameter of the pore and rotation angle of the nucleotide molecule with respect to the circular vacancy (see Figure 4b).

In Figure 5 we show the electronic results for the isolated pristine zigzag ribbon and its two other pore-structures. We set

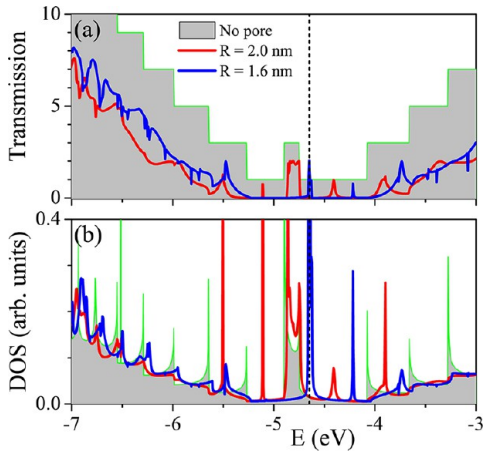

Figure 5. (a) Electronic transmission and (b) DOS as a function of energy (eV) for the pristine zigzag-edge nanoribbon of 4.5 nm in width (shadowed region) and for the same ribbon platform with holes of radius R_1 = 1.6 nm (blue line) and R_2 = 2.0 nm (red line). Vertical dashed line marks the Fermi energy of the pristine ribbon.

as a reference energy the Fermi level of the pristine zGNR which lays on $E_F = -4.65$ eV and it is marked by a vertical black line in the figure. As an overall, one can notice that the DOS is very pronounced in the vicinity of the reference Fermi energy for all pore configurations. This is reminiscent of the fact that all structures are derived from zigzag shaped-ribbons and it is well-known that they manifest metallic character ruled by 2-fold degenerate flat bands at the Fermi energy. However, most of these states have localized nature. This is confirmed through the transmission curves shown on the upper panel that are strongly suppressed around E_F for the pore systems. Their conductance profile is also highly dependent on their width. Besides the absolute value of the width itself, the way how atoms are arranged along the edge of the pore can dictate the transport response of the sensing platform. The hole can be composed of a combination of armchair and zigzag segments reinforcing even more the idea that the transport features of graphene nanopores are heavily correlated with the geometrical details of the central vacancy.[44]

After clarifying the electronic properties of isolated graphene nanopores, we are ready to place the DNA on their vacant section. Instead of a double strand, a single strand DNA (ss-DNA) containing 11 bp sequenced as GTGGCATAACG is positioned in such way that the carbon atom linking the phosphate and sugar is exactly on the center of the pore. In this way, we can capture the direct influence of each nucleotide on the transport properties of the graphene pore. The atomic structure was relaxed via conjugated gradient method assuming four different structural arrangements: (i) A-, (ii) T-, (iii) C-, or (iv) G nucleobase is aligned coplanar with the graphene pore. We imposed the constraint that at least the position of three nucleobase atoms, located right in the center of the pore, must be fixed in order to guarantee the coplanar arrangement between the molecule and the graphene sensor. After the successful relaxation, the electronic structure of the system is treated within SCC-DFTB with the DNA chain being truncated beyond second neighboring range. Such disruption will not significantly affect our results since the electronic coupling between the graphene and the DNA decreases exponentially with the length of the strand. At this point, it is also worth mentioning that effects emerged from DNA conformation along its translocation are not considered in this electronic study since they bring an uncertainty element to the detection procedure.[45,46] Here we limit our analysis to a system where one can achieve control over the DNA conformation in the pore as assumed by other theoretical works.[14,29] The transport properties are computed under steady state regime in which a snapshot of the fully relaxed atomic structure of the system is frozen. Subsequently, its optimized Hamiltonian is used to compute the electronic transmission at the Fermi level via Landauer formalism.[43] In order to provide a rough estimation on which range the transmission can fluctuate for a given nucleotide configuration coplanar to the graphene plane, we included an extra degree of freedom that is to rotate continuously the DNA molecule on the center of the pore.

We now present our analysis of the transport properties in graphene nanopore plus DNA by treating its electronic structure self-consistently. Upper panel of Figure 6 shows the transmission results for the system under neutral charged condition and a graphene pore of R_1 = 1.6 nm. As the DNA molecule rotates around z-axis perpendicular to the graphene plane, one can see that the electronic transmission fluctuates. The overall transmission is relatively small and its dispersion is rather smooth for all DNA nucleobases except for thymine. This occurs because one of the oxygen atoms in the radical $-PO_4$ for thymine base is positioned closer to the edges of pore than for other nucleotides. This can be better seen on the lower panel of the same figure which displays the minimum distance between the O atom (located on the upper part of the sensor) and the edge of pore as the molecule rotates. Each curve corresponds to a situation where a particular DNA nucleobase is aligned with the graphene plane. When thymine is aligned with the sensor plane, the separation between the DNA and the atoms along the pore circumference achieves the lowest values in comparison to the other nucleobases. This will render an asymmetric charge rearrangement that favors the electronic flow along the graphene. As a result, the transmission for thymine is approximately three times higher than for the other nucleobases. Thymine is hence the DNA nucleobase that our test graphene nanopore can discriminate better. Adenine also reveals a rather distinguishable electronic transmission but only at particular angles, ∼ 100 and ∼300°. Finally, cytosine and

dx.doi.org/10.1021/nl304735k | Nano Lett. 2013, 13, 1969−1976

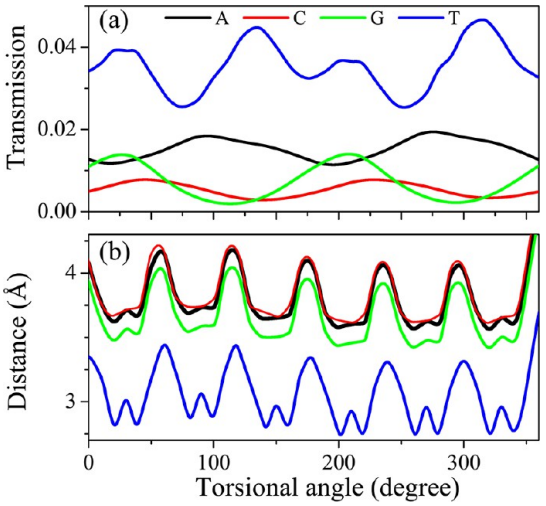

Figure 6. (a) Electronic transmission obtained at the Fermi energy of −4.65 eV as a function of the torsional angle for the nanopore with 1.6 nm in radius under neutral charge condition. Different DNA nucleotides are aligned with the graphene plane: adenine (black line), cytosine (red line), guanine (green line), and thymine (blue line). (b) Minimum distance between the edge of the pore and the respective nucleotides as a function of torsi onal angle.

guanine exhibit the lowest transmission rates and barely can be sensed by the graphene pore. We stress that for this calculation we chose a graphene pore with rather realistic diameters (at nanometer scale) and therefore a considerable spatial gap between the pore and the DNA exists. On top of that, since the pore platform is built from a zigzag nanoribbon, the transmission obtained at the Fermi energy has a major contribution coming from its zigzag edge state distributed along the outer extremes of the sensor. It is straightforward to think that the target molecule located in the pore will perturb even less such robust state. As a result, relative small disturbances in the transmission profiles are found because actually the DNA presence does not affect substantially the electronic charges on the extremities of the sensor. Obviously, the device looses even more effectiveness in identifying the distinct nucleotides as its diameter gets larger and larger.

Bearing in mind that DNA molecule is highly charged (one negative charge per phosphate deoxyribose), we repeated the calculations presented above assuming now that the system is negatively charged. Previous works have already pointed out the possibility of controlling the DNA dynamical translocation by charging not the DNA molecule but rather the graphene pore.[47] Here, an additional charge of −4e is considered for a DNA strand containing three bases standing in the vacant region of the sensor. Each PO_4 attached between the bases contributes with −1e and the PO_4 5′ end contributes with −2e. The transmission results are shown in Figure 7. The extra charges shift the energy levels of the DNA with respect to the Fermi level of the pore. As a consequence, the transmission values increase considerably for all aligned nucleotides. All the transmission curves oscillate approximately around 3.75 with adenine base displaying higher dispersions. The inclusion of charges in the system roughly leveled the transmission offset for all nucleotides making their detection even more complicated. A solution for this lack of selectiveness can be achieved when the transmission is conducted out of the Fermi energy associated with the robust zigzag edge state. By shifting the energy of the system by +0.2 eV away from the Fermi level, we

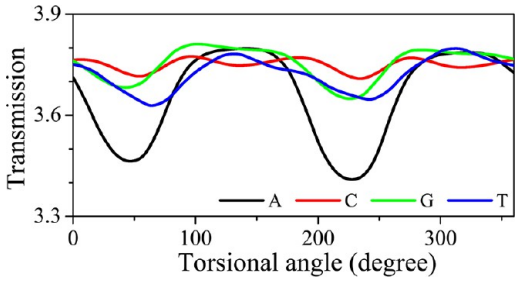

Figure 7. Electronic transmission obtained at the Fermi energy of −4.65 eV as a function of the torsional angle for the nanopore with 1.6 nm in radius under negative charge condition. Different DNA nucleotides are aligned with the graphene plane: adenine (black line), cytosine (red line), guanine (green line), and thymine (blue line).

resolve all four nucleobases in both neutral and charge conditions as displayed on Figure 8. This shift can be induced

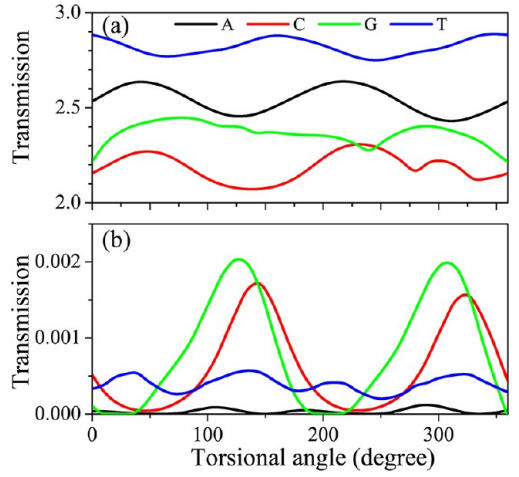

Figure 8. (a) Electronic transmission obtained at the energy of −4.45 eV ($E \rightarrow E_F$ + 0.2 eV) as a function of the torsional angle for the nanopore with 1.6 nm in radius under (a) neutral and (b) negative charge conditions. Different DNA nucleotides are aligned with the graphene plane: adenine (black line), cytosine (red line), guanine (green line), and thymine (blue line).

directly by a transversal electric field applied on the nanopore or by doping the graphene platform. Such a selective feature can also be observed from wave function plots obtained at the Γ point and at different energies. Figure 9 shows the wave functions calculated at the Fermi level for each nucleotide standing coplanar to the graphene pore plane. The DNA is set at neutral charge condition. One can notice that those states are very robust in response to the DNA presence. This picture is altered when the energy is tuned at −4.4 eV as depicted in Figure 10. Distinguishable patterns can be visualized from the wave function results demonstrating that each nucleobase can impart a signal on the sensor whether the energy is properly adjusted.

Conclusion. In summary, this work presents a detailed theoretical investigation about the sensing properties of graphene nanopores for sequencing DNA strands. Previous works somehow tend to overestimate the signal captured by the graphene pore as the DNA translocates through it. In particular, the reduced size of the pores used in the simulations is a prominent reason for capturing amplified electronic responses

dx.doi.org/10.1021/nl304735k | *Nano Lett.* 2013, 13, 1969−1976

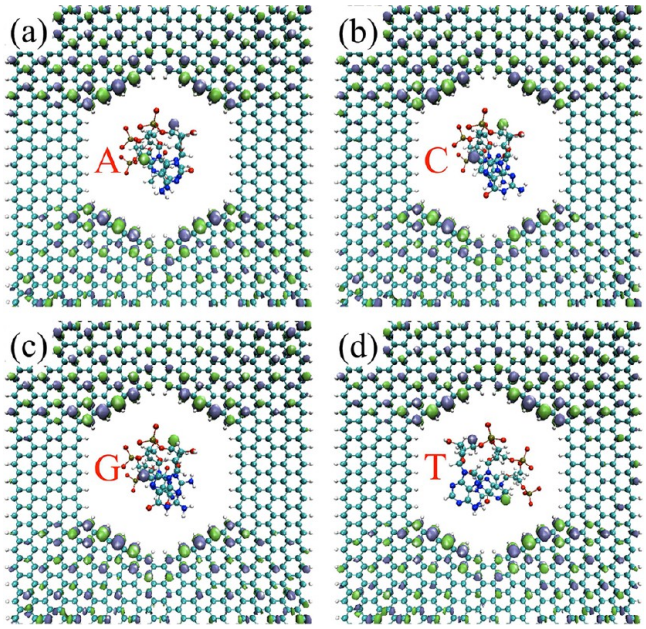

Figure 9. Wave function plots obtained at Γ-point and at the Fermi level for the respective nucleotides placed coplanar to the graphene pore plane: (a) adenine, (b) cytosine, (c) guanine, and (d) thymine.

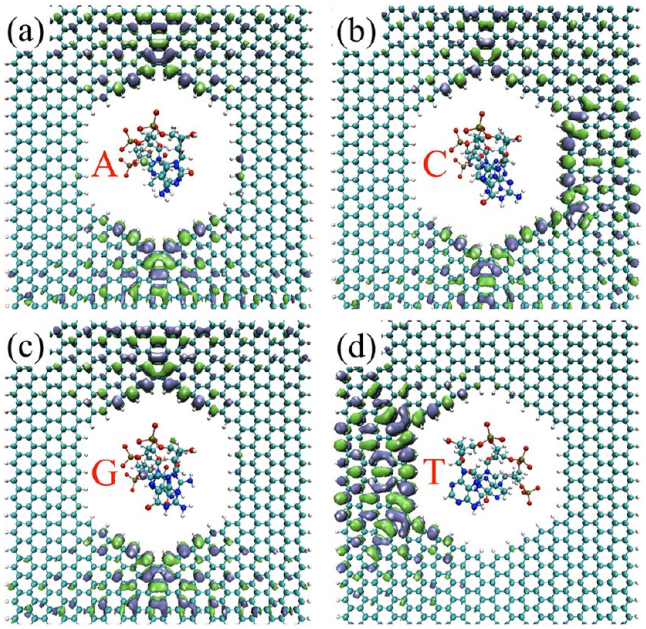

Figure 10. Wave function plots obtained at Γ-point and at the energy of −4.4 eV ($E \rightarrow E_F + 0.2$ eV) for the respective nucleotides placed coplanar to the graphene pore plane: (a) adenine, (b) cytosine, (c) guanine, and (d) thymine.

from the DNA.[29] While selecting graphene pores with nanometric sizes in diameter, the impact caused by the DNA on its transmission may be reduced. However, there are many other parameters that can be manipulated for achieving optimum responses even for nanopores of extended sizes. In particular, the atomic details of the graphene platform play an important role on the selectivity attributes of the devices. Platforms built from zigzag ribbons in particular have a drawback which is because its electronic structure at the Fermi level is characterized by a robust edge state. Our results reveal that it can be rather difficult to distinguish the DNA nucleobases while carrying the transmission along the pore at such energy state. In addition, the DNA charging conditions must also be taken into consideration in the calculations. By a simple energy shifting and assuming that the DNA can also be negatively charged, we obtained significant transport responses from the sensors even for nanopores with vacant areas reaching nanometer scales. In addition to electronic transport analysis, we also performed molecular dynamic studies in a distinct graphene nanopore setup containing four extra top graphene layers. This new detection architecture offers an alternative way of retarding the DNA translocation (besides the use of high viscosity fluids). It also reduces the kinetic movements of the carbon atoms located on the edge of the pore. In combination with a proper tuning of the electric field intensity, we obtained transient states in which the DNA molecule propagates through the pore with estimated velocities of approximately 17 bp/ns for an electric potential intensity of 2 V which is in excellent agreement with experimental results.

AUTHOR INFORMATION

Corresponding Author

*E-mail: claudia.c.gomes-darocha@phys.jyu.fi.

Author Contributions

S.A.M. performed the molecular dynamics simulations. D.N. performed the electronic transport calculations. C.G.R. wrote the manuscript and performed the wave function calculations. All authors discussed and commented on the manuscript and on the calculated results.

Notes

The authors declare no competing financial interest.

ACKNOWLEDGMENTS

We gratefully acknowledge the support provided from the German Excellence Initiative via the Cluster of Excellence EXC 1056 “Center for Advancing Electronics Dresden” (cfAED), European Union (European Social Fund), the Free State of Saxony (Sächsische Aufbaubank) in the young researcher group “InnovaSens” (SAB-Nr. 080942409), Volkswagen Foundation, Alexander von Humboldt Foundation, and The Academy of Finland. This research was also supported by World Class University program funded by the Ministry of Education, Science, and Technology through the National Research Foundation of Korea (R31-10100). We acknowledge the Center for Information Services and High Performance Computing (ZIH) at the Dresden University of Technology and CSC - IT Center for Science in Finland for the computational resources.

REFERENCES

(1) Crothers, D. M. *Principles of Nucleic Acid Structure*; Springer-Verlag: Berlin, 1984.
(2) Lander, E. S. *Nature* **2001**, *470*, 187.
(3) Mardis, E. R. *Nature* **2011**, *470*, 198.
(4) (a) Gilbert, W.; Maxam, A. *Proc. Natl. Acad. Sci. U.S.A.* **1973**, *70*, 3581. (b) Maxam, A. M.; Gilbert, W. *Proc. Natl. Acad. Sci. U.S.A.* **1977**, *74*, 560.
(5) Sanger, F.; Nicklen, S.; Coulson, A. R. *Proc. Natl. Acad. Sci. U.S.A.* **1977**, *74*, 5463.
(6) Kasianowicz, J. T.; Brandin, E.; Branton, D.; Deamer, D. W. *Proc. Natl Acad. Sci. U.S.A.* **1996**, *93*, 13770.
(7) Nakane, J. J.; Akeson, M.; Marzialli, A. *J. Phys.: Condens. Matter* **2003**, *15*, R1365.

(8) Fologea, D.; Gershow, M.; Ledden, B.; McNabb, D. S.; Golovchenko, J. A.; Li, J. *Nano Lett.* **2005**, *5*, 1905.
(9) Storm, A. J.; Storm, C.; Chen, J.; Zandbergen, H.; Joanny, J.-F.; Dekker, C. *Nano Lett.* **2005**, *5*, 1193.
(10) Wanunu, M.; Dadosh, T.; Ray, V.; Jin, J.; MacReynolds, L.; Drndić, M. *Nat. Nanotechnol.* **2010**, *5*, 807.
(11) Ivanov, A. P.; Instuli, E.; McGilvery, C. M.; Baldwin, G.; McComb, D. W.; Albrecht, T.; Edel, J. B. *Nano Lett.* **2011**, *11*, 279.
(12) Chang, H.; Kosari, F.; Andreadakis, G.; Alam, M. A.; Vasmatzis, G.; Bashir, R. *Nano Lett.* **2004**, *4*, 1551.
(13) Storm, A. J.; Chen, J. H.; Zandbergen, H. W.; Dekker, C. *Phys. Rev. E* **2005**, *71*, 051903.
(14) Gracheva, M. E.; Aksimentiev, A.; Leburton, J.-P. *Nanotechnology* **2006**, *17*, 3160.
(15) Venkatesan, B. M.; Shah, A. B.; Zuo, J.-M.; Bashir, R. *Adv. Funct. Mater.* **2010**, *20*, 1266.
(16) Chang, S.; et al. *Nano Lett.* **2010**, *10*, 1070.
(17) Postma, H. W. Ch. *Nano Lett.* **2010**, *10*, 420.
(18) Tsutsui, M.; Taniguchi, M.; Yokota, K.; Kawai, T. *Nat. Nanotechnol.* **2010**, *5*, 286.
(19) Guerrette, J. P.; Zhang, B. *J. Am. Chem. Soc.* **2010**, *132*, 17088.
(20) Nguyen, G.; Howorka, S.; Siwy, Z. S. *J. Membr. Biol.* **2011**, *239*, 105.
(21) (a) Novoselov, K. S.; et al. *Science* **2004**, *306*, 666. (b) Novoselov, K. S.; et al. *Nature* **2005**, *438*, 197.
(22) Rocha, C. G.; et al.; *Graphene: Synthesis and Applications*; Taylor and Francis, LLC: New York, 2011; Chapter 1.
(23) Garaj, S.; Hubbard, W.; Reina, A.; Kong, J.; Branton, D.; Golovchenko, J. A. *Nature* **2010**, *467*, 190.
(24) Schneider, G. F.; et al. *Nano Lett.* **2010**, *10*, 3163.
(25) Merchant, C. A.; et al. *Nano Lett.* **2010**, *10*, 2915.
(26) Branton, D.; et al. *Nat. Biotechnol.* **2008**, *26*, 1146.
(27) Min, S. K.; Kim, W. Y.; Cho, Y.; Kim, K. S. *Nat. Nanotechnol.* **2011**, *6*, 162.
(28) Saha, K. K.; Drndić, M.; Nikolić, B. K. *Nano Lett.* **2012**, *12* (12), 50.
(29) Nelson, T.; Zhang, B.; Prezhdo, O. V. *Nano Lett.* **2010**, *10*, 3237.
(30) Siwy, Z. S.; Davenport, M. *Nat. Natechnol.* **2010**, *5*, 697.
(31) Wells, D. B.; Belkin, M.; Comer, J.; Aksimentiev, A. *Nano Lett.* **2012**, *12*, 4117.
(32) Li, J.; Talaga, D. S. *J. Phys.: Condens. Matter* **2010**, *22*, 454129.
(33) Shi, Z.; Yang, R.; Zhang, L.; Wang, Y.; Liu, D.; Shi, D.; Wang, E.; Zhang, G. *Adv. Mater.* **2011**, *23*, 3061.
(34) Humphrey, W.; Dalke, A.; Schulten, K. Vmd: Visual molecular dynamics. *J. Mol. Graph.* **1996**, *14*, 33.
(35) Kalé, L.; Skeel, R.; Bhandarkar, M.; Brunner, R.; Gursoy, A.; Krawetz, N.; Phillips, J.; Shinozaki, A.; Varadarajan, K.; Schulten, K. Namd2: Greater scalability for parallel molecular dynamics. *J. Comput. Phys.* **1999**, *151*, 283.
(36) Brooks, B. R.; et al. *J. Comput. Chem.* **1983**, *4*, 187.
(37) Wang, J.; Wolf, R. M.; Caldwell, J. W.; Kollman, P. A.; Case, D. A. *J. Comput. Chem.* **2004**, *25*, 1157.
(38) Jorgensen, W. L.; Chandrasekhar, J.; Madura, J. D.; Impey, R. W.; Klein, M. L. *J. Chem. Phys.* **1983**, *79*, 926.
(39) Pedretti, A.; Villa, L.; Vistoli, G. *J. Mol. Graph. Model.* **2002**, *21*, 47.
(40) Schlick, T. *Molecular Modeling and Simulation*; Springer: New York, 2002, pp 435−438..
(41) *DFTB+: Density Functional based Tight Binding (and more)*; http://www.dftb-plus.info and *The DFTB website*; http://www.dftb.org.
(42) Elstner, M.; Porezag, D.; Jungnickel, G.; Elsner, J.; Haugk, M.; Frauenheim, T.; Suhai, S.; Seifert, G. *Phys. Rev. B* **1998**, *58*, 7260.
(43) Datta, S. *Electronic Transport in Mesoscopic Systems*; Cambridge University Press: Cambridge, 1995.
(44) Rosales, L.; Pacheco, M.; Barticevic, Z.; León, A.; Latgé, A.; Orellana, P. A. *Phys. Rev. B* **2009**, *80*, 073402.
(45) Heng, J. B.; et al. *Nano Lett.* **2005**, *5*, 1883.
(46) Sigalov, G.; et al. *Nano Lett.* **2008**, *8*, 56.
(47) Sathe, C.; Zou, X.; Leburton, J.-P.; Schulten, K. *ACS Nano* **2011**, *5*, 8842.